Ingeniería Mecánica en España - Mechanical Engineering in Spain - Research Article

Analysis of the backward bending modes in damped rotating beams

Jose Martínez-Casas[1] , Francisco David Denia[1], Juan Fayos Sancho[2,3],
Enrique Nadal Soriano[1] and Juan Giner-Navarro[1]

Abstract

This article presents a study of the backward bending mode of a simply supported rotating Rayleigh beam with internal damping. The study analyses the natural frequency behaviour of the backward mode according to the internal viscous damping ratio, the slenderness of the beam and its spin speed. To date, the behaviour of the natural frequency of the backward mode is known to be a monotonically decreasing function with spin speed due to gyroscopic effects. In this article, however, it is shown that this behaviour of the natural frequency may not hold for certain damping and slenderness conditions, and reaches a minimum value (concave function) from which it begins to increase. Accordingly, the analytical expression of the spin speed for which the natural frequency of the backward mode attains the minimum value has been obtained. In addition, the internal damping ratio and slenderness intervals associated with such behaviour have been also provided.

Keywords

Backward bending mode, damped rotating Rayleigh beam, natural frequency behaviour, Campbell diagram, internal viscous damping ratio, slenderness

Introduction

There have been numerous publications in the field of rotor dynamics over the past 50 years. Although some of these works have focused on modelling the dynamic behaviour,[1–6] most of them have paid attention to natural frequencies, mode shapes, critical speeds, thresholds of instability and unbalanced response.[7–24] The stability studies have been related to the potentially unstable forward bending mode while the analysis of the stable backward mode has been overlooked. However, in the field of railway dynamics, recent works have shown that the dynamics associated with certain backward bending modes of a wheelset are important in order to describe various relevant phenomena. Vila et al.[25] showed that a wavelength-fixing mechanism of rail corrugation is due to the excitation of some backward bending modes, where the roughness growth is predicted on the low rail for specific vehicle circulation conditions in curve. In addition, regarding the squeal noise phenomenon, Glocker et al.[26] concluded that the excitation of certain wheel mode shapes is responsible for the squeal noise generation mechanism (also wheel modal coupling). Thus, to gain a further insight into

[1]Centro de Investigación en Ingeniería Mecánica, Universitat Politècnica de València, Valencia, Spain
[2]Departamento de Ingeniería Mecánica y de Materiales, Universitat Politècnica de València, Valencia, Spain
[3]Comet Ingeniería, Valencia, Spain

Corresponding author:
Jose Martínez-Casas, Centro de Investigación en Ingeniería Mecánica, Universitat Politècnica de València, Camino de Vera, s/n, 46022 Valencia, Spain.
Email: jomarc12@mcm.upv.es

the physics of the problem, the backward bending mode is studied in the current work.

The literature related to the stability of rotating shafts differs according to the basic model adopted in the formulation (Jeffcott, Euler, Rayleigh or Timoshenko), the effects and properties considered (rotational inertia, gyroscopic effects, shear deformation and the type of internal and external damping) and the boundary conditions. It is well known that the classical Euler beam is not suitable for studying the dynamic behaviour of rotating beams. The rotational inertia and gyroscopic effects, included, for example, in the Rayleigh beam model, must be taken into account as shown by Sheu and Yang[7] and Sheu[8] in their studies of the stability of undamped rotating beams under various boundary conditions. For even greater precision, the couplings caused by shear deformation (as shown for the Timoshenko model)[9,10] can also be considered.

A study of internally damped rotating shafts was first made by Kimball.[11] This study revealed the destabilizing effect of internal friction due to bending in the supercritical range, although the type of damping used was not specified. This phenomenon was demonstrated later by Dimentberg[12] for viscous internal damping, as well as in works listed in Genin and Maybee,[13] and Zorzi and Nelson.[14] Internal damping, also known as rotary damping, has been modelled as viscous and hysteretic damping. Its influence on the stability of the rotating system for both models has been analysed and compared in detail in different works. These comparisons have used Timoshenko models through an analytical approach[15] for several boundary conditions, as well as numerical simulations using finite elements.[14,16] These studies mainly conclude that internal viscous damping has a destabilizing effect once the synchronous speed is reached, unlike hysteretic damping which has a destabilizing effect at any speed. However, later Genta,[17] using Jeffcott and Timoshenko models, and Montagnier and Hochard,[18] applying a Rayleigh model, conclude that hysteretic damping only destabilizes once synchronous speed is reached, in the same way as viscous damping. Other studies regarding the influence of internal viscous damping on the stability of rotors are given in Dimentberg[19] and Vatta F and Vigliani[20] for a Jeffcott rotor, the former study considering a random variation of damping and the latter discussing a non-linear damping model. Rosales and Filipich[21] and Mazzei and Scott[22] take into account the gyroscopic effects of rotational inertia in the Rayleigh model and agree on the fact that the destabilizing effect arises once critical speed is reached.

The presence of external damping, also known as non-rotary damping, differs from internal damping as it has a stabilizing effect at any speed, as demonstrated in studies by Ehrich,[23] and subsequently by Vance and Lee[24] and Zorzi and Nelson,[14] and more recently in the research works[16,18,22] for Rayleigh and Timoshenko beam models. All these studies have concluded that the introduction of external damping using rolling bearings and hydrodynamic bearings results in a stable range within supercritical motion, and so improves system stability.

Most of the publications on the study of rotor stability cited previously concluded that the backward bending mode is stable for all speeds, slenderness and internal damping,[3,14,16,18,19,27] and that only the forward bending mode is able to cause instability.[3,14,16–19] In the Campbell diagram of the backward mode shown in the research works,[3,9,10,16,18,21,22,28–34] it can be seen that natural frequencies monotonically decrease with spin speed due to gyroscopic effects. However, this behaviour cannot be held for certain damping and slenderness conditions, since a minimum value can be reached as it will be evidenced in this article. Specifically, in the absence of internal damping, the natural frequency of the backward mode decreases monotonically with spin speed. Many articles[3,9,10,21,22,28–34] demonstrate that this is the expected behaviour, and it will be proved analytically later. However, in the presence of internal viscous damping, the behaviour may change, that is, the natural frequency can behave as if the system was undamped (decreasing function) as shown in the studies,[3,16,18,21] or it can have a minimum threshold from which it begins to increase. Such behaviour of increasing natural frequency has hardly been addressed in the literature. Genta[3] and Lee[35] showed a slightly increasing trend considering a Jeffcott model, as well as Ku[16] and Montagnier and Hochard,[18] who adopted a rotating Rayleigh beam model. Further research on the reasons for this change in the Campbell diagram (spin speed, internal damping, slenderness) is carried out in the context of the current work.

Thus, for a simply supported rotating Rayleigh beam with internal damping, this article presents an analytical study of the behaviour of the natural frequency of the backward bending mode with respect to the spin speed (Campbell diagram), the internal viscous damping ratio and the slenderness of the beam. Rotational inertia and gyroscopic effects are taken into account in order to analytically formulate the sign change suffered by the slope of the natural frequency curve (minimum value). The analytical expression of the spin speed associated with this minimum value has been obtained, as well as the internal damping ratio and slenderness intervals where it occurs. Once this spin speed is formulated, a comparison is made with the critical speed of the forward mode to demonstrate the validity of the current work.

One-dimensional model of the Rayleigh beam

In this section, the formulation associated with the one-dimensional simply supported Rayleigh beam model,

including rotation and internal modal viscous damping, is summarized. Further details can be found in Genta.[3]

The kth mass normalized bending mode calculated in the neutral axis of the Rayleigh beam is

$$\varphi_k(z) = \frac{1}{\sqrt{m_k}} \sin\left(\frac{k\,\pi\,z}{L}\right) \qquad (1)$$

where the constant m_k has the following expression

$$m_k = \frac{\rho\,A\,L}{2} + \frac{\rho\,I\,(k\,\pi)^2}{2\,L} \qquad (2)$$

The transverse displacements are computed from the fixed frame through the following modal approach

$$\begin{Bmatrix} x(z,t) \\ y(z,t) \end{Bmatrix} = \sum_{k=1}^{\infty} \varphi_k(z) \begin{Bmatrix} q_x^k(t) \\ q_y^k(t) \end{Bmatrix} = \sum_{k=1}^{\infty} \varphi_k\, \mathbf{q}^k \qquad (3)$$

where $\mathbf{q}^k$ is the two-dimensional vector with modal coordinate associates with the kth orthogonal bending mode shape. The equation of motion for the damped simply supported rotating Rayleigh beam in modal coordinates is

$$\ddot{\mathbf{q}}^k + 2\left(\Omega\,g_k\,\mathbf{G} + c_k\,\mathbf{I}\right)\dot{\mathbf{q}}^k + \left(\omega_k^2\,\mathbf{I} + 2\,\Omega\,c_k\,\mathbf{G}\right)\mathbf{q}^k = \mathbf{Q}^k \qquad (4)$$

where $\mathbf{Q}^k$ being the generalized external force, $\mathbf{I}$ the identity matrix 2×2, Ω the beam spin speed and ω_k the natural frequency of the kth bending mode of the simply supported non-rotary Rayleigh beam.[36–38] The term c_k is computed from the internal modal damping ratio of the kth bending mode ξ_k as

$$c_k = \omega_k\xi_k \qquad (5)$$

The modal gyroscopic term g_k is obtained from the following expression

$$g_k = \frac{(k\,\pi)^2}{\lambda^2 + (k\,\pi)^2} \qquad (6)$$

where g_k is bounded between 0 and 1, and λ is the slenderness of the beam. Matrix $\mathbf{G}$ is skew-symmetric matrix and couples both orthogonal bending modes. It is expressed as follows

$$\mathbf{G} = \begin{pmatrix} 0 & 1 \\ -1 & 0 \end{pmatrix} \qquad (7)$$

The equation of motion (4) can be written as

$$\ddot{\mathbf{q}}^k + 2\begin{pmatrix} c_k & \Omega\,g_k \\ -\Omega\,g_k & c_k \end{pmatrix}\dot{\mathbf{q}}^k + \begin{pmatrix} \omega_k^2 & 2\,\Omega\,c_k \\ -2\,\Omega\,c_k & \omega_k^2 \end{pmatrix}\mathbf{q}^k = \mathbf{Q}^k \qquad (8)$$

where the eigenvalues of the previous equation are

$$\beta_{k,1} = -c_k + i\,g_k\,\Omega + \sqrt{c_k^2 - \omega_k^2 - g_k^2\,\Omega^2 - 2\,i\,\Omega\,c_k\,(g_k - 1)}$$

$$\beta_{k,2} = -c_k + i\,g_k\,\Omega - \sqrt{c_k^2 - \omega_k^2 - g_k^2\,\Omega^2 - 2\,i\,\Omega\,c_k\,(g_k - 1)}$$

$$\beta_{k,3} = \beta_{k,1}^*$$

$$\beta_{k,4} = \beta_{k,2}^*$$

$$(9)$$

The notation z^* represents the complex conjugate of z, $\beta_{k,1}$ and $\beta_{k,3}$ are the eigenvalues for the forward mode and $\beta_{k,2}$ and $\beta_{k,4}$ are associated with the backward mode.

Study of the behaviour of the backward bending mode of a damped simply supported rotating Rayleigh beam

Once the equation of motion for a damped simply supported rotating Rayleigh beam has been shown, the next step is to analyse the dynamic behaviour of the backward bending mode in terms of the slenderness of the beam, internal viscous damping ratio and the spin speed. The ultimate aim is to describe analytically the change in sign suffered by the slope of its natural frequency. In this study, only the backward mode eigenvalues are considered.

Stability analysis

The eigenvalues of the forward and backward bending modes are computed in equation (9). As a criterion for studying the stability of the system, one can choose to analyse the logarithmic decrement in the system response (an approach taken by Zorzi and Nelson,[14] Ku[16] and Montagnier and Hochard[18]) or the real part of the eigenvalues (Routh's criterion). The latter option has been adopted here: the condition for the stability of the system being that all the eigenvalues have strictly negative real part. This criterion was used by Melanson and Zu[15] and Mazzei and Scott[22] when studying the stability of an internally damped shaft. If the backward mode eigenvalues described in equation (9) are observed, their real part is always negative, that is

$$\mathrm{Re}(\beta_{k,2}) < 0, \quad \mathrm{Re}(\beta_{k,4}) < 0 \quad \forall\Omega \qquad (10)$$

so the backward modes are stable at all speeds, for any value of internal viscous damping and slenderness (represented by g_k). This is in agreement with the literature[3,14,16,18,19,27] and it is reflected in Figure 1(a), where the real part of the backward mode is monotonically decreasing. If the internal damping is considered as hysteretic or structural, Zorzi and Nelson[14] and Genta[17] also demonstrate that the backward mode is always stable.
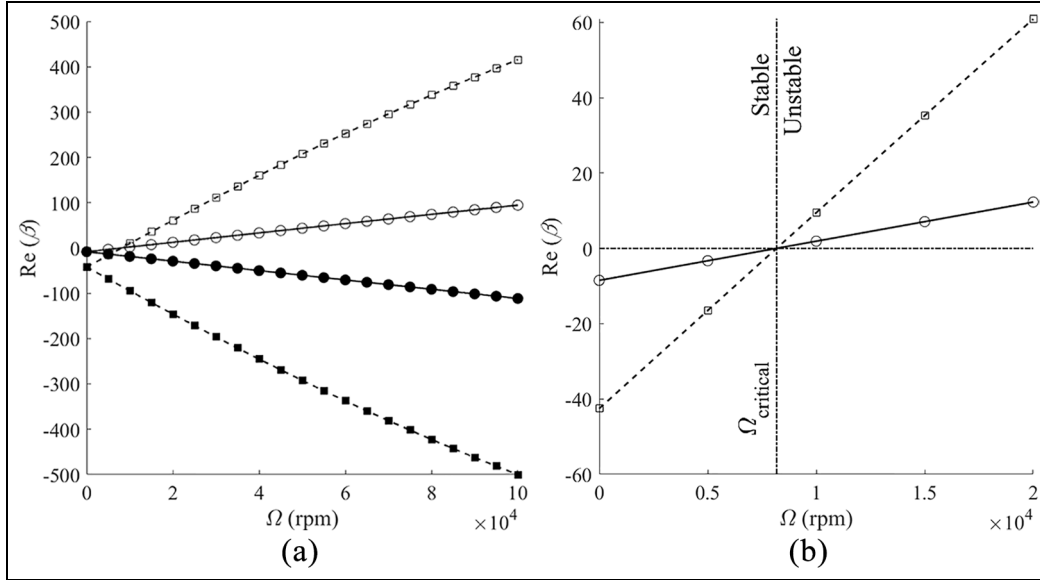
Figure 1. Real part of the eigenvalues for $\lambda = 40$. ○—○ and ●—●, forward and backward modes, respectively, with $\xi = 1\%$; ▱▱ and ■—■, forward and backward modes, respectively, with $\xi = 5\%$.

However, the forward modes reveal a critical speed beyond which the real part of their eigenvalues is positive and hence unstable

$$\Omega_k^{\mathrm{critical}} = \frac{\omega_k}{\sqrt{1 - 2\,g_k}} \qquad (11)$$

This shows that if there is no external damping as in the case under study, then the critical speed is independent of the internal damping ratio, a conclusion also made by Melanson and Zu.[15] Consequently, equation (11) is the same critical speed expression calculated by Sheu and Yang[7] in their study of the stability of undamped rotating Rayleigh beams.

Figure 1(a) shows that the real part of the eigenvalues of the forward mode is monotonically growing and the backward mode is monotonically decreasing for spin speed. This performance has been previously noted in the literature.[3,15,16,21] Accordingly, the real part of the forward mode reaches positive values once the critical spin speed is achieved, as it is shown in Figure 1(b), where the critical speed is independent of the internal damping ratio in the absence of external damping. Moreover, without external damping and a spin speed $\Omega_k^{\mathrm{critical}}$, the absolute value of the imaginary part of the eigenvalues of the kth forward bending mode is given by

$$\Omega = \Omega_k^{\mathrm{critical}} = \frac{\omega_k}{\sqrt{1 - 2\,g_k}} \quad \Rightarrow$$
$$\left| \mathrm{Im}\left(\beta_{k,1}\right) \right| = \left| \mathrm{Im}\left(\beta_{k,3}\right) \right| = \Omega_k^{\mathrm{critical}} \qquad (12)$$

which means that, in the absence of external damping, the instability starts when the spin speed equals that of

the forward mode. This conclusion was reached by Genta,[3] Sheu and Yang,[7] and Ku[16] for the finite element model of a Timoshenko beam, and by Vatta and Vigliani[20] using a non-linear approach for internal damping. Genta[17] made the same conclusion when considering non-viscous hysteretic damping and studied the stability of a Jeffcott rotor and a simply supported Timoshenko beam.

In the presence of external damping, the critical speed is greater than that of forward bending mode because the external damping stabilizes the system, while internal damping destabilizes the system.[3,14,16,18,22,24,27] Specifically, as shown in Figure 1(b), internal viscous damping stabilizes for speeds below the critical one and destabilizes for faster speeds. This is in agreement with the literature.[3,13–15,21,22] Genta[17] shows that internal hysteretic damping behaves similarly.

Natural frequencies

In the previous section, the real part of the eigenvalues of forward and backward modes has been shown to be monotonically increasing and decreasing, respectively.[3,15,16,21] A different trend is found, however, for the imaginary part of the eigenvalues associated with the backward mode, as it is shown below. In this section, the imaginary part of the eigenvalues (natural frequencies) is studied. The analysis focuses on the backward bending mode with a view to providing a detailed description of the sign change related to the slope of the corresponding natural frequency (minimum of the curve), the associated spin speed at which
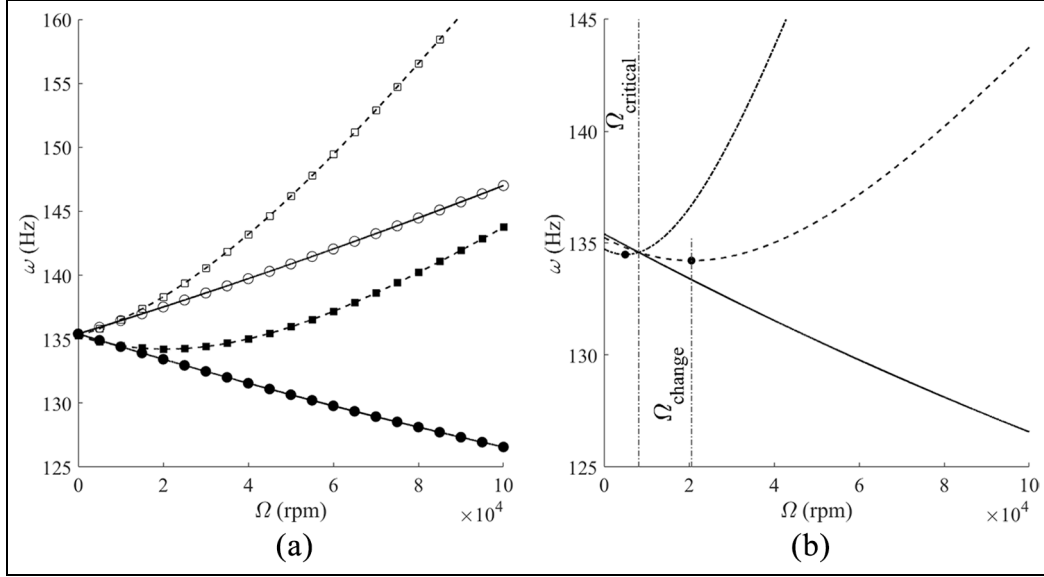
Figure 2. Campbell diagram for $\lambda = 40$. (a) ∘—∘ and •—•, forward and backward modes, respectively, with $\xi = 1\%$; ⊡⊡and ■ ■, forward and backward modes, respectively, with $\xi = 5\%$. (b) backward mode: ——, $\xi = 1\%$; — —, $\xi = 5\%$; – –, $\xi = 10\%$.

the sign change appears and the corresponding conditions of slenderness and damping ratios.

The eigenvalues for the forward and backward bending modes can be computed from equation (9), and their imaginary parts are, respectively, given as follows (see Appendix 1)

$$\mathrm{Im}(\beta_{k,1}) = f_1(\xi, \lambda, \Omega) = g_k\Omega$$
$$+ \sqrt{\frac{1}{2}\left[\sqrt{(c_k^2 - \omega_k^2)^2 + g_k^4\Omega^4 - 2c_k^2 g_k^2\Omega^2 + 2\omega_k^2 g_k^2\Omega^2 + 4\Omega^2 c_k^2(g_k-1)^2} - c_k^2 + \omega_k^2 + g_k^2\Omega^2\right]}$$

$$(13)$$

$$\mathrm{Im}(\beta_{k,2}) = f_2(\xi, \lambda, \Omega) = g_k\Omega$$
$$- \sqrt{\frac{1}{2}\left[\sqrt{(c_k^2 - \omega_k^2)^2 + g_k^4\Omega^4 - 2c_k^2 g_k^2\Omega^2 + 2\omega_k^2 g_k^2\Omega^2 + 4\Omega^2 c_k^2(g_k-1)^2} - c_k^2 + \omega_k^2 + g_k^2\Omega^2\right]}$$

where, if the internal damping is neglected, the same expressions are found for the natural frequencies of the rotating Rayleigh beam compared to those obtained by Sheu and Yang[7] and Sheu[8] when considering rotary inertia and gyroscopic effects.

Figure 2(a) shows the natural frequencies of the first forward and backward bending modes according to spin speed Ω (Campbell diagram), for various internal damping ratios ξ and a slenderness of the beam $\lambda = 40$. As can be seen in this figure, the imaginary part of the eigenvalue associated with the forward mode is monotonically increasing with spin speed for both internal viscous damping ratios. This behaviour has been known for years and it is discussed in the literature.[3,15,16,18,21] In the case of hysteretic internal damping, the natural

frequency of the forward mode exhibits the same trend, as shown in Genta[17] and Montagnier and Hochard[18] and even in the absence of internal damping as indicated in the research works.[3,7–9,21,22,28–34,39] The natural frequency of the backward bending mode shows a very different behaviour, as can be observed in Figure 2(a) and (b). Unlike the forward mode, the natural frequency of the backward mode is not always monotonically decreasing with the spin speed.[3,16,18,35] Moreover, a curve minimum is found for certain internal damping and slenderness conditions. If there is no internal damping, the natural frequency of the backward mode decreases monotonically with spin speed.[3,9,10,21,22,28–34] This behaviour without internal damping is expected and has been known for years. However, in the presence of internal damping, the evolution of the natural frequency corresponding to the backward mode can change and shows a minimum for certain damping and slenderness values. This behaviour is shown in Figure 2(a). For the damping ratio $\xi = 1\%$, the natural frequency of the backward mode is monotonically

decreasing (as in the internally undamped case) and this behaviour has been shown by other authors.[3,16,18,21] However, $\xi = 5\%$ damping ratio reveals a curve minimum. This phenomenon will be studied in depth below as it is the main objective of this article.
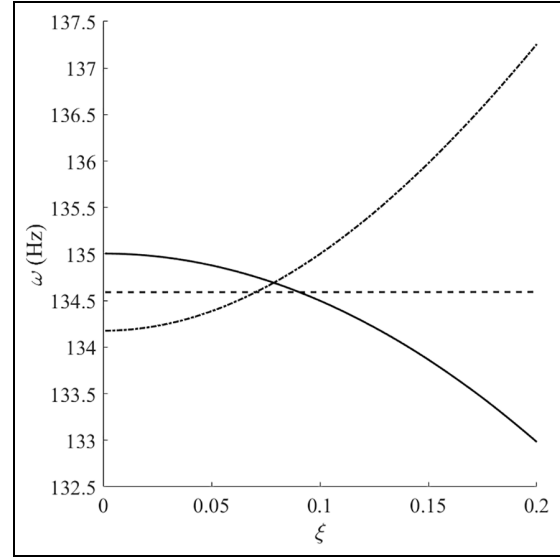
Figure 2(b) shows the natural frequency of the first backward mode for various internal damping ratios. It can be clearly seen that for a value $\xi = 1\%$, the curve is monotonically decreasing, unlike the cases with $\xi = 5\%$ and $\xi = 10\%$ where the corresponding functions are no longer monotonically decreasing but concave. Accordingly, a minimum value appears (see black dot) at a spin speed termed Ω_{change} from which the natural frequency shows a positive slope and begins to increase. The spin speed Ω_{change} depends on the slenderness and internal viscous damping ratio of the beam, and it may be lower or higher than the critical speed $\Omega_{\mathrm{critical}}$ of forward mode as shown in Figure 2(b).

As previously mentioned, the aim of this article is to study in detail the behaviour of the natural frequency for the backward mode. To achieve this goal, the analytical expression for the spin speed that produces the sign change in its slope $\Omega_k^{\mathrm{change}}(\xi_k, \lambda)$ (and therefore the curve minimum) will be obtained. In addition, an assessment is provided of the damping ratio and slenderness conditions under which this phenomenon occurs.

Dependence of the natural frequency of the backward bending mode on the internal damping ratio. This section studies the influence of the internal damping ratio ξ on the natural frequency of the backward mode, $\omega_{k,2} = \mathrm{Im}(\beta_{k,2})$. The derivative of the imaginary part of the eigenvalue defined in equation (13) with respect to the damping ratio is set equal to zero in order to find the minimum (see Appendix 1). This yields

$$\frac{\partial \mathrm{Im}(\beta_{k,2})}{\partial \xi_k} = \frac{\partial \omega_{k,2}}{\partial \xi_k} = 0 \quad \Leftrightarrow$$
$$\Omega = \Omega_k^{\mathrm{critical}} = \frac{\omega_k}{\sqrt{1 - 2g_k}} \quad , \quad \forall \xi_k \tag{14}$$

Accordingly, when the spin speed of the beam coincides with the critical speed of the forward mode, the natural frequency of the backward mode does not depend on the damping ratio. This is shown in Genta[3] and can be also seen in Figure 2(b) for the critical speed where all curves intersect at one point. The same occurs for the forward bending mode at this critical speed. If the spin speed is less than the critical value, the natural frequency of the backward mode will be monotonically decreasing, and if it is higher than critical speed, then the natural frequency will be monotonically increasing, as shown in Figure 3.

Figure 3. Natural frequency of the first backward bending mode for $\lambda = 40$. ——, $\Omega < \Omega_1^{\mathrm{critical}}$; — —, $\Omega = \Omega_1^{\mathrm{critical}}$; – –, $\Omega > \Omega_1^{\mathrm{critical}}$.

This behaviour of the natural frequency of the backward mode with respect to the internal damping ratio can be described mathematically as follows

$$\Omega < \Omega_k^{\mathrm{critical}} \quad \Rightarrow \quad \frac{\partial \mathrm{Im}(\beta_{k,2})}{\partial \xi_k} = \frac{\partial \omega_{k,2}}{\partial \xi_k} < 0$$
$$\text{monotone decreasing}$$

$$\Omega = \Omega_k^{\mathrm{critical}} \quad \Rightarrow \quad \frac{\partial \mathrm{Im}(\beta_{k,2})}{\partial \xi_k} = \frac{\partial \omega_{k,2}}{\partial \xi_k} = 0 \tag{15}$$
$$\text{constant function}$$

$$\Omega > \Omega_k^{\mathrm{critical}} \quad \Rightarrow \quad \frac{\partial \mathrm{Im}(\beta_{k,2})}{\partial \xi_k} = \frac{\partial \omega_{k,2}}{\partial \xi_k} > 0$$
$$\text{monotone increasing}$$

Behaviour of the natural frequency of the backward bending mode as a function of the spin speed. This section analyses the behaviour of the natural frequency of the kth backward bending mode with respect to the spin speed. As shown in Figure 2, the natural frequency of the backward mode reaches a minimum value from which it begins to increase. The numerical values involved depend on the slenderness and damping ratio. As in the previous section, to determine the minimum of the curve, the derivative of the imaginary part of the backward mode (see equation (13)) with respect to the spin speed is computed and set equal to zero. This yields the spin speed $\Omega_k^{\mathrm{change}}$ for which the slope changes its sign

$$\frac{\mathrm{d}\,\mathrm{Im}(\beta_{k,2})}{\mathrm{d}\Omega} = \frac{\mathrm{d}\omega_{k,2}}{\mathrm{d}\Omega} = 0 \quad \Rightarrow \quad \Omega_k^{\mathrm{change}} = f(\xi_k, \lambda) \tag{16}$$

From equation (16), the following sixth-degree polynomial is obtained for spin speed (see Appendix 1)

$$A_k \Omega^6 + B_k \Omega^4 + C_k \Omega^2 + D_k = 0 \quad \leftarrow$$
$$\text{Exact polynomial} \tag{17}$$

The roots of equation (17) provide the spin speeds Ω_k^{change} for which the natural frequency of the backward mode reaches a minimum.

The sixth-degree polynomial could be reduced to a third degree with a simple change of variable. However, the analytic solution of the real root (Ω_k^{change}) is complicated and unwieldy due to the complex expressions of the polynomial coefficients. The terms in Ω^6 and Ω^4 have been found to be negligible compared to the rest, so the sixth-degree polynomial (equation (17)) can be simplified to a fourth degree by ignoring the coefficient A and to a second degree by ignoring the coefficients A and B. Although it is not detailed in the document, a study of singular perturbation in the fourth-degree polynomial has been carried out in order to justify the second-degree simplification proposed. The associated error will be evaluated next to validate this simplification. The simplified polynomials can be written as

$$B_k \Omega^4 + C_k \Omega^2 + D_k = 0$$
$$\text{Simplified fourth} - \text{degree polynomial} \tag{18}$$

$$C_k \Omega^2 + D_k = 0$$
$$\text{Simplified second} - \text{degree polynomial} \tag{19}$$

where the fourth- and second-degree polynomials have analytical solutions.

To represent the spin speed $\Omega_1^{\text{change}}(\xi_1, \lambda)$ where the natural frequency of the first backward mode reaches the minimum value, a parametric sweep of the internal damping ratio and the slenderness of the beam are made for the three polynomials. The ratio between the radius of the beam and its length, $r = R/L$, is considered as a representative parameter of the slenderness (this also contributes to the improvement of the graphic representations). The following terms are defined

$$\lambda(r) = \frac{2}{r} \tag{20}$$

$$g_1(r) = \frac{\pi^2}{\frac{4}{r^2} + \pi^2} \tag{21}$$

$$\omega_1(r) = \sqrt{\frac{E \pi^4}{\rho L^2 \left(\frac{4}{r^2} + \pi^2\right)}} \tag{22}$$

where λ is the slenderness of the beam, g_1 is the modal gyroscopic term of the first bending mode and ω_1 is the natural frequency of the first bending mode of the non-rotary simply supported Rayleigh beam. The geometric

Table 1. Beam properties.

|	
Length	$L = 1.5\,\text{m}$
Radius-to-length ratio (variable)	$r = \dfrac{R}{L} = [0.002 \cdots 0.2]$
Mode index	$k = 1$
Density	$\rho = 7800\,\text{kg/m}^3$
Young's modulus	$E = 2.1 \times 10^{11}\,\text{N/m}^2$
Internal damping ratio (variable)	$\xi = [0 \cdots 0.2]$
Poisson's ratio	$\nu = 0.3$

and material properties are defined in Table 1, as well as the range of the two parametric variables considered in the study.

Once the properties of the Rayleigh beam and the polynomials (equations (17)–(19)) have been defined, the spin speed $\Omega_1^{\text{change}}(\xi_1, \lambda)$ is plotted for the three different polynomials through a sweep of the ratios ξ and r (inversely proportional to slenderness), as shown in Figures 4 and 5.

Figure 4(a) shows the spin speed for which the minimum value of the natural frequency of the backward mode is reached versus the parameter $r = R/L$. The influence of different viscous internal damping ratios is also included in the figure. For a specific damping ratio, it is seen that spin speed Ω_1^{change} increases when the slenderness of the beam is reduced (or when r increases). This magnitude reveals an asymptotic behaviour to infinity for a critical value of slenderness that depends on the ratio of internal damping. This critical value is termed the 'numerical critical slenderness' for the one associated with the sixth-degree polynomial (numerical solution) and 'analytical critical slenderness' for the one associated with the second-degree polynomial (analytical solution). It is important to clarify the nomenclature because, although the term 'numerical critical slenderness' is associated with the sixth-degree polynomial (which is solved numerically), it nevertheless represents an 'exact' critical slenderness. This is different to what happens with 'analytical critical slenderness' calculated from the simplified second-degree polynomial.

So, for a fixed damping ratio, if the slenderness of the beam is greater than the critical slenderness, then the natural frequency of the backward mode reveals a minimum value from which it begins to increase, and so the curve is a concave function. However, if the slenderness is equal to or lower than the critical slenderness, then the natural frequency of the backward mode is a monotonically decreasing function, in the same way as its real part. It can also be seen that the greater the damping ratio, the greater the slenderness domain where the natural frequency minimum is reached.

Figure 5(a) shows again the same magnitude but, in this case, compared with the internal viscous damping ratio for various values of slenderness. For a fixed
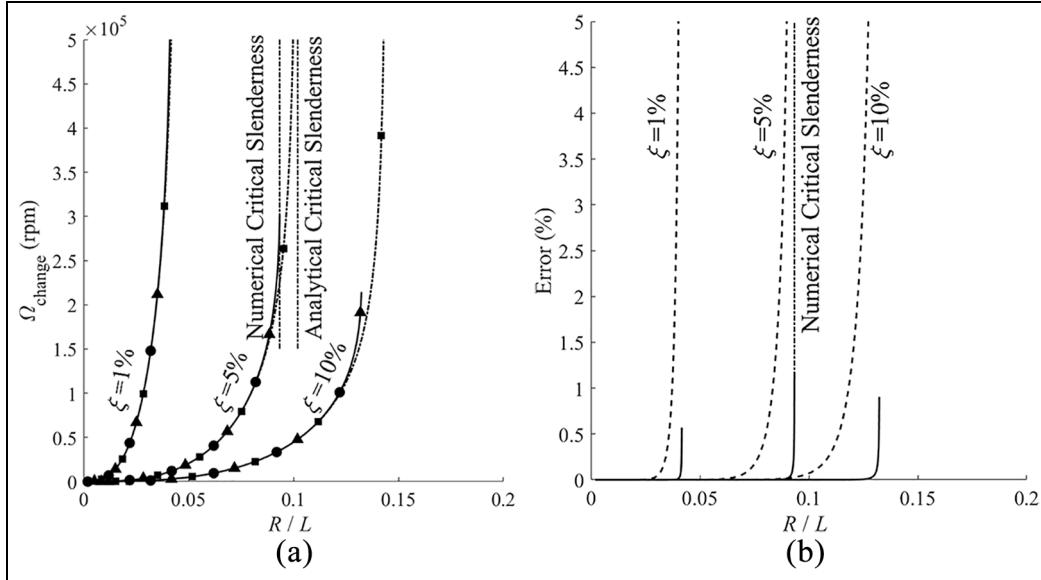
Figure 4. (a) Spin speed for which the natural frequency of the first backward mode reaches the minimum value: ●—●, sixth-degree polynomial; ▲--▲, fourth-degree polynomial; ■-··-■, second-degree polynomial. (b) Relative error in same magnitude: ——, fourth-degree polynomial compared to sixth-degree polynomial; - - - - -, second-degree polynomial compared to sixth-degree polynomial.

slenderness, the spin speed Ω_1^{change} decreases with the damping ratio, and an asymptotic behaviour to infinity for a critical value of damping ratio can be seen again. As before, the critical value of damping ratio is termed 'analytical' or 'numerical' critical damping depending on the polynomial under consideration.

Therefore, if the damping ratio is equal to or less than the critical ratio, then the natural frequency will

$$
\Omega_k^{\text{change}}(\lambda, \xi_k) = g_k\, \omega_k \left(1 - {\xi_k}^2\right)
$$
$$
\times \sqrt{\frac{1 - {\xi_k}^2}{{\xi_k}^4\left({g_k}^4 - 10\,{g_k}^3 + 9\,{g_k}^2 - 4\,g_k + 1\right) + {\xi_k}^2\left(3\,{g_k}^4 + 6\,{g_k}^3 - 3\,{g_k}^2\right) - 3\,{g_k}^4}} \tag{23}
$$

not reach a minimum value and it will be a monotonically decreasing function. However, if the damping ratio is greater than the critical value, then there will be a natural frequency minimum and the function will be concave. It is worth noting that the greater the slenderness of the beam, the wider the damping ratio domain where the natural frequency of backward mode reaches a minimum value.

Figures 4(b) and 5(b) show the relative error made by simplifying the original sixth-degree polynomial to fourth- and second-degree ones. Both figures show that the error is negligible across the entire domain, except when approaching the critical value where the error tends to infinity, in the same way as spin speed Ω_1^{change}. Similar to the solution of sixth-degree polynomial, the analytical solution of the fourth-degree polynomial is

complicated and unwieldy due to the complex expressions of the polynomial coefficients. Therefore, a second-degree polynomial can be used to calculate the spin speed at which the minimum value of the natural frequency is reached (zero slope) in situations not too close to the critical values. The real root of the second-degree polynomial (equation (19)) can be analytically written as follows

Before continuing with the study, it is worth analysing what happens when there is no internal viscous damping ($\xi_k = 0\%$). If the internal damping ratio is cancelled in equation (23), the spin speed Ω_k^{change} turns out to be a complex number, and so the natural frequency of the backward mode is monotone decreasing with the spin speed. This is consistent with the results shown in the research works[3,9,10,21,22,28–34] for the undamped case.

To complete the study of the natural frequency behaviour associated with the backward mode, the critical values of slenderness and damping ratio, reflected in Figures 4 and 5, respectively, must be analysed. These values determine whether or not a minimum value of the natural frequency is reached with the spin speed. Figures 4(a) and 5(a) show that for each damping ratio, there is a critical slenderness and vice versa.
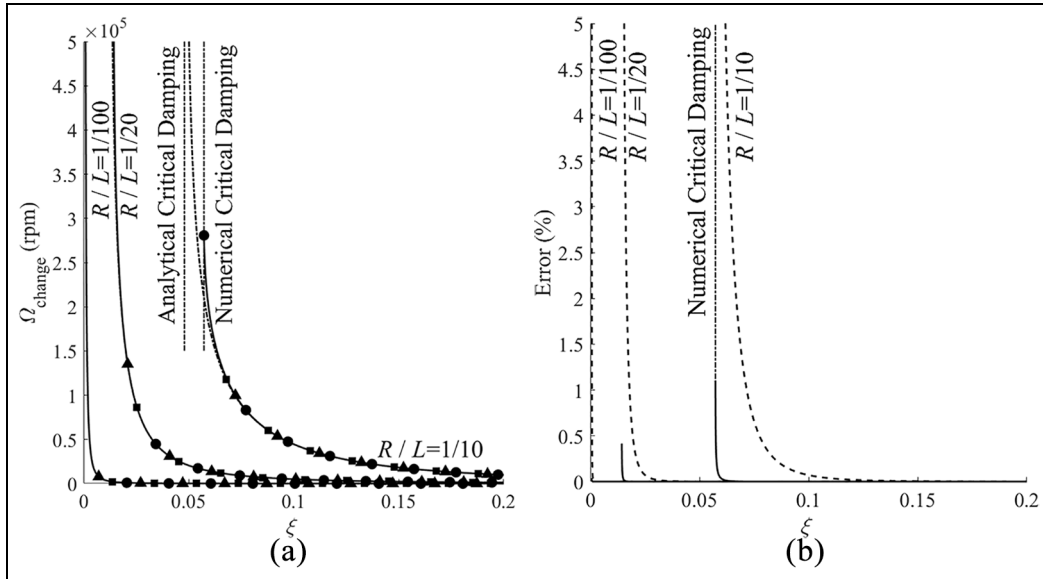
Figure 5. (a) Spin speed for which the natural frequency of the first backward mode reaches the minimum value: ●—●, sixth-degree polynomial; ▲---▲, fourth-degree polynomial; ■---■, second-degree polynomial. (b) Relative error in same magnitude: ——, fourth-degree polynomial compared to sixth-degree polynomial; - - - - -, second-degree polynomial compared to sixth-degree polynomial.
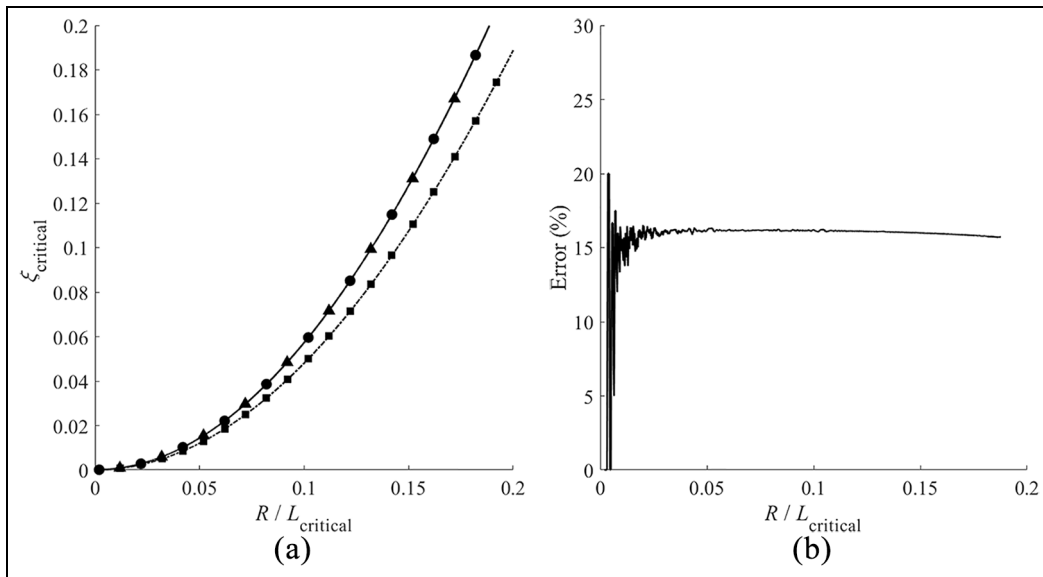
Figure 6. (a) Critical internal damping ratio: ●—●, sixth-degree polynomial; ▲--▲, fourth-degree polynomial; ■---■, second-degree polynomial. (b) Relative error: ——, second-degree polynomial compared to sixth degree.

Figure 6(a) shows the critical damping ratio depending on the slenderness of the beam for the three polynomials considered. The sixth polynomial has been calculated numerically, while the solutions of the fourth- and second-degree polynomials have been computed analytically. It can be seen that the critical damping ratio increases with the parameter r; accordingly, the greater the slenderness, the lower the critical damping ratio and the greater the internal damping ratio domain where the natural frequency reaches a minimum value.

The behaviour of the fourth-degree polynomial solution is very similar to that associated with the sixth-degree polynomial. However, more relevant discrepancies are found when the second-degree polynomial is considered, as shown in Figure 6(b). It can be observed that the difference between the numerical critical damping ratio (sixth-degree polynomial) and the analytical critical damping ratio (second-degree polynomial) is nearly constant, with an approximate value of 16%. Therefore, it is possible to obtain a semi-analytical
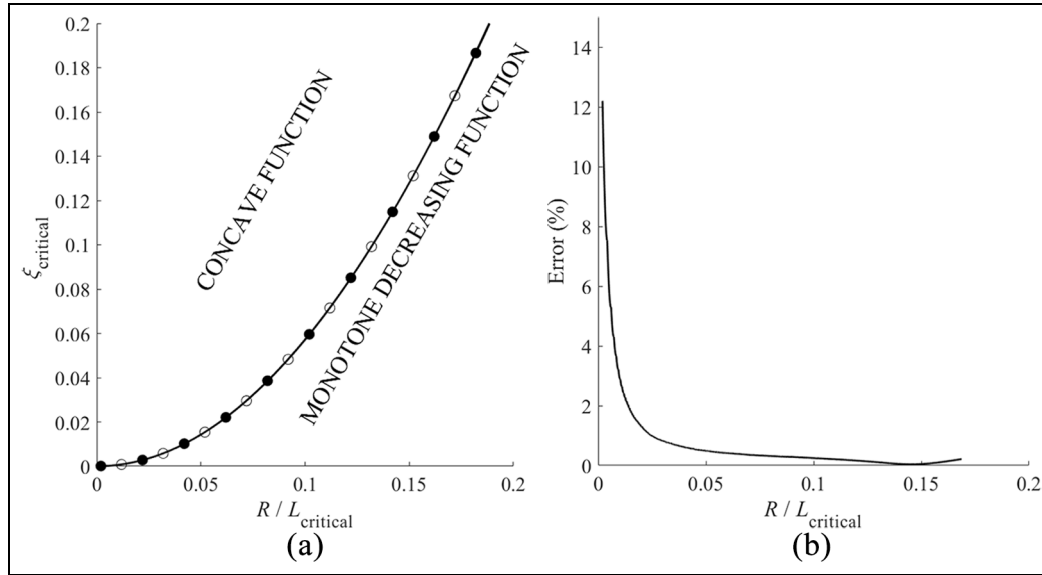
Figure 7. (a) Critical internal damping ratio for sixth-degree polynomial: •—•, numerical critical damping ratio; ∘—∘, semi-analytical critical damping ratio. (b) ——, relative error between both magnitudes.

expression for the critical damping ratio of the sixth-degree polynomial from the second-degree polynomial plus a correction factor.

The analytical critical damping ratio of the second-degree polynomial is given by the following expression (see Appendix 1)

$$\xi^{\text{critical}}_{k,\,\text{degree 2}}(\lambda) = g_k \sqrt{\frac{\sqrt{21} - 3}{2\,g_k{}^2 + \left(2\,\sqrt{21} - 10\right) g_k + 5 - \sqrt{21}}} \tag{24}$$

Taking into account the aforementioned correction factor yields

$$\xi^{\text{critical}}_{k,\,\text{degree 6}}(\lambda) = \frac{100}{84}\,g_k$$
$$\times \sqrt{\frac{\sqrt{21} - 3}{2\,g_k{}^2 + \left(2\,\sqrt{21} - 10\right) g_k + 5 - \sqrt{21}}} \tag{25}$$

where $\xi^{\text{critical}}_{k,\,\text{degree 6}}$ being the semi-analytical critical damping ratio of the kth backward bending mode of the sixth-degree polynomial, which is estimated from the analytical solution of the second-degree polynomial.

To validate the last expression, Figure 7(a) represents the numerical critical damping ratio of the sixth-degree polynomial and the semi-analytical critical damping ratio calculated from equation (25).

It can be seen that the numerical and semi-analytical critical damping ratio curves of the sixth-degree polynomial are almost undistinguishable curves with a very small discrepancy in most of the domain (see Figure 7(b)). Therefore, the semi-analytical critical damping

ratio $\xi^{\text{critical}}_{k,\,\text{degree 6}}$ defined in equation (25) is validated from a practical point of view. It is worth pointing out again that according to Figure 7(a), the greater the slenderness of the beam (lower r), the lower the critical damping ratio and the greater the internal damping ratio domain where the natural frequency of the backward mode reaches a minimum value.

Finally, a comparison is carried out between the spin speed Ω^{change}_k where the natural frequency of the backward mode reaches a minimum value with the critical spin speed $\Omega^{\text{critical}}_k$ of the forward mode from which it becomes unstable. The aim is to examine if the spin speed Ω^{change}_k exceeds the critical spin speed of the forward mode and the conditions of damping ratio and slenderness for this to occur.

Figure 8(a) shows that the greater the internal damping ratio, the wider the interval domain of the beam slenderness in which the spin speed Ω^{change}_k is lower than the critical speed of the forward mode. The same applies to slenderness, because according to Figure 8(b), the greater the slenderness, the wider the damping ratio domain where the minimum frequency of the backward mode is reached at speeds below the critical one, that is, without destabilizing the forward bending mode. Therefore, there are intervals of slenderness and damping ratio where the minimum natural frequency of the backward mode is reached without actually destabilizing the forward mode, thereby justifying the importance of the study on backward mode.

If the slenderness of the beam and its internal damping ratio are known, the speed ratio can be evaluated analytically as follows
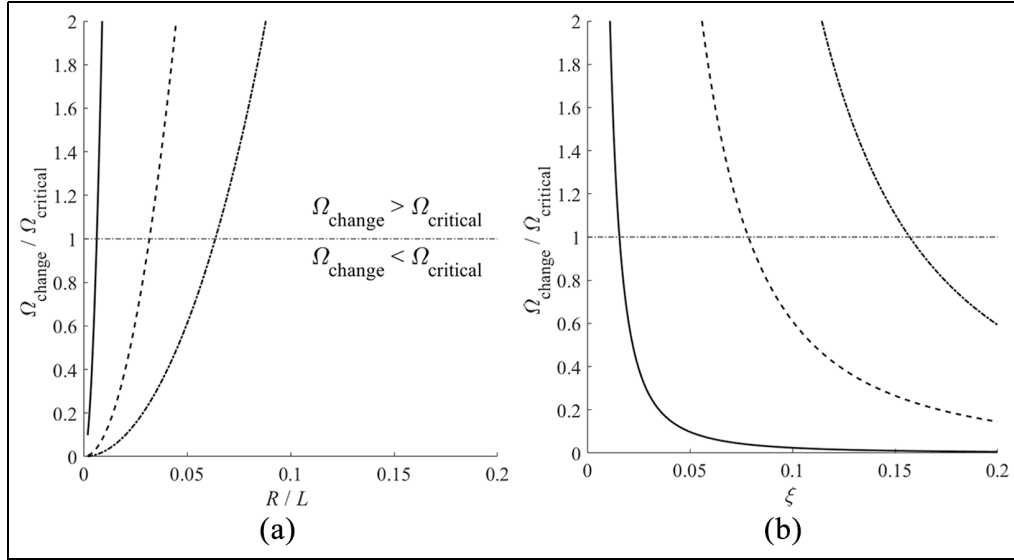
Figure 8. Ratio of the spin speed for which the natural frequency of the first backward mode reaches the minimum value to the critical spin speed of the forward mode. (a) ——, $\xi = 1\%$; — —, $\xi = 5\%$; – –, $\xi = 10\%$. (b) ——, $r = 1/100$; — —, $r = 1/20$; – –, $r = 1/10$.

$$
\begin{aligned}
ratio_k(\lambda, \xi_k) &= \frac{\Omega_k^{\text{change}}(\lambda, \xi_k)}{\Omega_k^{\text{critical}}(\lambda)} \\
&= g_k \sqrt{\frac{(1 - 2g_k)(1 - \xi_k^2)^3}{\xi_k^4(g_k^4 - 10g_k^3 + 9g_k^2 - 4g_k + 1) + \xi_k^2(3g_k^4 + 6g_k^3 - 3g_k^2) - 3g_k^4}}
\end{aligned}
\tag{26}
$$

If $ratio_k < 1$, then the minimum frequency of backward mode is reached before the forward mode is destabilized, unlike the case $ratio_k > 1$ where it is necessary to destabilize the forward mode to reach the minimum natural frequency associated with the backward mode.

Conclusion

In this article, an analytical formulation to assess the behaviour of natural frequency of the backward bending mode of a simply supported rotating Rayleigh beam with internal damping has been developed. Results are presented confirming that the behaviour of the natural frequency of the backward mode is not always monotone decreasing, as it has been commonly reported in the literature for the undamped case. It has been shown here that if the beam is internally damped, then the natural frequency can reach a minimum value.

The ultimate aim of this work has been to determine the spin speed at which the minimum natural frequency for backward mode is reached, and to analyse the conditions of slenderness and internal viscous damping for this phenomenon to occur. The influence of the internal damping ratio on the natural frequency has been analysed in detail, and a relationship has been found with the critical speed of the forward mode. To evaluate the conditions leading to the minimum value of the natural frequency of backward mode, the influence of spin speed has been studied. The damping ratio and slenderness intervals where the natural frequency reaches a minimum value have been also analysed through the critical damping ratio. It can be concluded that the greater the beam slenderness, the lower the critical damping ratio, and therefore the natural frequency of the backward mode is more likely to reach a minimum value. Moreover, a speed ratio has been defined to determine if the minimum natural frequency occurs before or after the forward mode is destabilized.

Declaration of conflicting interests

The author(s) declared no potential conflicts of interest with respect to the research, authorship, and/or publication of this article.

Funding

ORCID iD

Jose Martínez-Casas   https://orcid.org/0000-0001-5706-4951

References

1. Brown MA and Shabana AA. Application of multibody methodology to rotating shaft problems. *J Sound Vib* 1997; 204: 439–457.
2. Shabana AA. *Dynamics of multibody systems*. 3rd ed. Cambridge, Cambridge University Press, 2005.
3. Genta G. *Dynamics of rotating systems*. New York: Springer, 2005.
4. Fayos J, Baeza L, Denia FD, et al. An Eulerian coordinate-based method for analysing the structural vibrations of a solid of revolution rotating about its main axis. *J Sound Vib* 2007; 306: 618–635.
5. Martínez-Casas J, Fayos J, Denia FD, et al. Dynamics of damped rotating solids of revolution through an Eulerian modal approach. *J Sound Vib* 2012; 331: 868–882.
6. Martínez-Casas J, Di Gialleonardo E, Bruni S, et al. A comprehensive model of the railway wheelset-track interaction in curves. *J Sound Vib* 2014; 333: 4152–4169.
7. Sheu GJ and Yang SM. Dynamic analysis of a spinning Rayleigh beam. *Int J Mech Sci* 2005; 47: 157–169.
8. Sheu GJ. On the hollowness ratio effect on the dynamics of a spinning Rayleigh beam. *Int J Mech Sci* 2007; 49: 414–422.
9. Zu JWZ and Han RPS. Natural frequencies and normal modes of a spinning Timoshenko beam with general boundary conditions. *J Appl Mech* 1992; 59: 197–204.
10. Chen LW and Peng WK. Stability analyses of a Timoshenko shaft with dissimilar lateral moments of inertia. *J Sound Vib* 1997; 207: 33–46.
11. Kimball AL. Internal friction theory of shaft whirling. *General Electr Rev* 1924; 27: 244–251.
12. Dimentberg MF. *Flexural vibrations of rotating shafts*. London: Butterworths, 1961.
13. Genin J and Maybee JS. The role of material damping in the stability of rotating systems. *J Sound Vib* 1971; 21: 399–404.
14. Zorzi ES and Nelson HD. Finite element simulation of rotor-bearing systems with internal damping. *J Eng Power* 1977; 99: 71–76.
15. Melanson J and Zu JW. Free vibration and stability analysis of internally damped rotating shafts with general boundary conditions. *J Vib Acoust* 1998; 120: 776–783.
16. Ku DM. Finite element analysis of whirl speeds for rotor-bearing systems with internal damping. *Mech Syst Signal Pr* 1998; 12: 599–610.
17. Genta G. On a persistent misunderstanding of the role of hysteretic damping in rotordynamics. *J Vib Acoust* 2004; 126: 459–461.
18. Montagnier O and Hochard CH. Dynamic instability of supercritical driveshafts mounted on dissipative supports – effects of viscous and hysteretic internal damping. *J Sound Vib* 2007; 305: 378–400.
19. Dimentberg MF. Vibration of a rotating shaft with randomly varying internal damping. *J Sound Vib* 2005; 285: 759–765.
20. Vatta F and Vigliani A. Internal damping in rotating shafts. *Mech Mach Theory* 2008; 43: 1376–1384.
21. Rosales MB and Filipich CP. Dynamic stability of a spinning beam carrying an axial dead load. *J Sound Vib* 1993; 163: 283–294.
22. Mazzei AJ and Scott RA. Effects of internal viscous damping on the stability of a rotating shaft driven through a universal joint. *J Sound Vib* 2003; 265: 863–885.
23. Ehrich FF. Shaft whirl induced by rotor internal damping. *J Appl Mech* 1964; 31: 279–282.
24. Vance JM and Lee J. Stability of high speed rotors with internal friction. *J Eng Ind* 1974; 96: 960–968.
25. Vila P, Baeza L, Martínez-Casas J, et al. Rail corrugation growth accounting for the flexibility and rotation of the wheel set and the non-Hertzian and non-steady-state effects at contact patch. *Vehicle Syst Dyn* 2014; 52: 92–108.
26. Glocker CH, Cataldi-Spinola E and Leine RI. Curve squealing of trains: measurement, modelling and simulation. *J Sound Vib* 2009; 324: 365–386.
27. Den Hartog JP. *Mechanical vibrations*. New York: Dover Publication, 1985.
28. Bauer HF. Vibration of a rotating uniform beam, part I: orientation in the axis of rotation. *J Sound Vib* 1980; 72: 177–189.
29. Shiau TN and Hwang JL. Generalized polynomial expansion method for the dynamic analysis of rotor-bearing systems. *J Eng Gas Turb Power* 1993; 115: 209–217.
30. Yu J and Craggs A. 3-D solid finite element modeling of rotating shafts. In: *Proceedings of the 15th international modal analysis conference (IMAC)*, vols I and II, Orlando, FL, 3–6 February 1997, pp.1488–1494. Berlin: SEM.
31. Hili MA, Fakhfakh T and Haddar M. Vibration analysis of a rotating flexible shaft-disk system. *J Eng Math* 2007; 57: 351–363.
32. Young TH, Shiau TN and Kuo ZH. Dynamic stability of rotor-bearing systems subjected to random axial forces. *J Sound Vib* 2007; 305: 467–480.
33. Wang J, Hurskainen V, Matikainen MK, et al. On the dynamic analysis of rotating shafts using nonlinear super-element and absolute nodal coordinate formulations. *Adv Mech Eng* 2017; 9: 1–14.
34. Ran S, Hu Y and Wu H. Design, modeling, and robust control of the flexible rotor to pass the first bending critical speed with active magnetic bearing. *Adv Mech Eng* 2017; 10: 1–13.
35. Lee CW. *Vibration analysis of rotors*. Berlin: Springer, 1993.

36. Weaver W Jr, Timoshenko SP and Young DH. *Vibration problems in engineering.* 5th ed. New York: Wiley, 1990.
37. Shabana AA. *Theory of vibration* (Volume II: discrete and continuous systems). New York: Springer, 1991.
38. Genta G. *Vibration of structures and machines, practical aspects.* 3rd ed. New York: Springer, 1999.
39. Cheng CC and Lin JK. Modelling a rotating shaft subjected to a high-speed moving force. *J Sound Vib* 2003; 261: 955–965.

Appendix 1

The eigenvalues of the simply supported Rayleigh beam are given by equation (9). If the next expression is considered

$$\mathrm{Im}\left(\sqrt{a + i\,b}\right) = \sqrt{\frac{1}{2}\left(\sqrt{a^2 + b^2} - a\right)} \qquad (27)$$

where the constants are the given by

$$\begin{aligned} a &= c_k^2 - \omega_k^2 - g_k^2\,\Omega^2 \\ b &= -2\,\Omega\,c_k\,(g_k - 1) \end{aligned} \qquad (28)$$

Then, equation (13) is derived from equations (27) and (28).

The imaginary part of the eigenvalue associated with the backward bending mode given by equation (13) is derived with respect to the internal damping ratio. Equating to zero yields

$$\begin{aligned} & c_k^2 - \omega_k^2 + \Omega^2\left(2 + g_k^2 - 4\,g_k\right) \\ & = \sqrt{\left(c_k^2 - \omega_k^2\right)^2 + g_k^4\,\Omega^4 - 2\,c_k^2\,g_k^2\,\Omega^2 + 2\,\omega_k^2\,g_k^2\,\Omega^2 + 4\,\Omega^2\,c_k^2\,(g_k - 1)^2} \end{aligned} \qquad (29)$$

Squaring both sides of equation (29) leads to

$$\Omega^2\left(-2\,g_k^3 + 5\,g_k^2 - 4\,g_k + 1\right) = \omega_k^2\left(g_k^2 - 2\,g_k + 1\right) \qquad (30)$$

where the internal damping ratio has been cancelled. If the spin speed is computed from equation (30), equation (14) is proved.

If the imaginary part of the eigenvalues corresponding to the backward bending mode (equation (13)) is derived in terms of the spin speed, and the derivative is set equal to zero, equation (17) is proved. The polynomial coefficients are the following

$$\begin{aligned} A_k &= a_k'^2 - d_k'^2\,f_k' \\ B_k &= 2\,a_k'\,b_k' - d_k'^2\,g_k' - 2\,d_k'\,e_k'\,f_k' \\ C_k &= b_k'^2 + 2\,a_k'\,c_k' - d_k'^2\,h_k' - 2\,d_k'\,e_k'\,g_k' - f_k'\,e_k'^2 \\ D_k &= 2\,c_k'\,b_k' - 2\,d_k'\,e_k'\,h_k' - e_k'^2\,g_k' \end{aligned} \qquad (31)$$

with the notation

$$\begin{aligned} a_k' &= 2\,g_k^6\left(c_k^2 - \omega_k^2\right) \\ b_k' &= 4\left[c_k^4\left(g_k^4 - 6\,g_k^3 + 7\,g_k^2 - 4\,g_k + 1\right)\right. \\ &\quad \left. + g_k^2\,c_k^2\,\omega_k^2\left(g_k^2 + 2\,g_k - 1\right) - g_k^4\,\omega_k^4\right] \\ c_k' &= 2\,g_k^2\left(c_k^6 + 3\,c_k^2\,\omega_k^4 - 3\,c_k^4\,\omega_k^2 - \omega_k^6\right) \\ d_k' &= 2\,g_k^2\left[c_k^2\left(g_k^2 - 4\,g_k + 2\right) + g_k^2\,\omega_k^2\right] \\ e_k' &= 2\,g_k^2\left(c_k^2 - \omega_k^2\right)^2 \\ f_k' &= g_k^4 \\ g_k' &= -2\,c_k^2\,g_k^2 + 2\,\omega_k^2\,g_k^2 + 4\,c_k^2\,(g_k - 1)^2 \\ h_k' &= \left(c_k^2 - \omega_k^2\right)^2 \end{aligned} \qquad (32)$$

The second-degree polynomial defined in equation (19) defines the spin speed where the natural frequency of the backward mode reaches a minimum value. This provides

$$\Omega_k^{\mathrm{change}} = \sqrt{\frac{-D_k}{C_k}} \qquad (33)$$

and therefore

$$\Omega_k^{\mathrm{change}} \to \infty \quad \Leftrightarrow \quad C_k \to 0 \qquad (34)$$

so the condition for the spin speed $\Omega_k^{\mathrm{change}}$ to tend to infinity is that the denominator tends to zero. This latter condition yields, after suitable manipulation, the expression of the critical damping ratio defined in equation (24).